



Porosity evolution and diagenetic history of the upper Jurassic Mozduran Formation, eastern Kopet-Dagh Basin, NE Iran

Mehdi Reza Poursoltani*, Mahin Harati-Sabzvar

Department of Geology, Mashhad Branch, Islamic Azad University, Mashhad, Iran

Received 18 September 2018; accepted 9 January 2019

Abstract

The Upper Jurassic carbonates of the eastern part of the Kopet-Dagh Basin, with thickness of 470 m, are the major gas-bearing reservoir in NE Iran. The objectives of this study are recognition of diagenetic history and estimation of porosity related to dolomitization. Based on field and laboratory study, four carbonate facies associations have been identified at the Mazdavand outcrop. Most of the carbonate rocks were deposited in an open marine, tidal channel and barrier, lagoon and tidal flat setting. Using petrographic and CL analyses, the main diagenetic processes that affected these rocks are micritization, cementation, compaction, fracturing, dissolution, neomorphism, silicification, and dolomitization. Dissolution of grains and calcite cement generated secondary porosity, whereas compaction and cementation are the primary cause of porosity reduction. The average porosity of core plugs is 15.78% and match well with two-dimensional estimates from thin sections. The more porous samples are either highly fractured or contain interparticle and intercrystalline porosity, within the lower strata that contain more dolostone.

Keywords: *porosity, diagenesis, carbonate, Mozduran Formation, Iran*

1. Introduction

The Mesozoic to Cenozoic collision between the Eurasian and the Afro-Arabian plates and its influence on the geologic and tectonic setting in Iran has been discussed by a large number of geologists from different points of views (e.g. Stöcklin 1968; Berberian 1976; Jackson et al. 1995; Allen et al. 2004; Reilinger et al. 2006; Vernant and Chery 2006; Kaviani et al. 2009; Kargaranbafghi et al. 2011). Because of the enormous hydrocarbon potential of strata laid down during these events, mountain ranges and associated sedimentary basins resulting from this collision, such as the Zagros mountains and the Alborz and the Kopet-Dagh basins, have been the focus of numerous studies (Fig 1) (Bretis et al. 2012).

The Kopet-Dagh Basin of northeast Iran, is an inverted basin (Allen et al. 2003) extending from the east of the Caspian Sea to NE Iran, Turkmenistan and north Afghanistan (Afshar Harb 1979; Buryakovsky et al. 2001). This basin separates Central Iran from the Turan plate (Jackson et al. 2002). Following the closure of Palaeo-Tethys in the Middle Triassic (Alavi et al. 1997) and the opening of Neo-Tethys during the Early to Middle Jurassic (Buryakovsky et al. 2001), the Kopet-Dagh Basin formed in an extensional regime during the Early to Middle Jurassic (Garzanti and Gaetani 2002). This successor basin accumulated 7 km of post-Triassic strata (Moussavi Harami and Brenner 1992), after which the strata were uplifted and deformed during Cenozoic

collisional events along the southern Asian margin (Lyberis and Manby 1999). Jurassic-Cenozoic carbonates and siliciclastics unconformably overlie Palaeozoic (basement) and Triassic rocks (Ulmishek 2004). The Jurassic Mozduran Formation is composed principally of limestones and dolomites with minor marl/shales, sandstones and evaporites, and crops out along the Kopet-Dagh Range where it forms a reservoir rock (Kavoossi et al. 2009). Mozduran Formation was deposited on a carbonate platform developed across the elongate Kopet-Dagh Basin (Lasemi 1995).

The major reservoir in the giant Khangiran gas field in the Kopet-Dagh Basin is a highly porous and permeable dolomitic interval of the Upper Jurassic (Oxfordian–Kimmeridgian) Mozduran Formation (Mahboubi et al. 2010). These carbonate rocks grade laterally to coarser siliciclastic and evaporite sediments in the Agh-Darband area in the easternmost parts of the basin (Moussavi Harami 1989; Zand Moghadam et al. 2016). The Lower Cretaceous Shurijeh Formation comprising siliciclastic deposits is also considered a reservoir in the basin.

The major source rock interval occurs in the Middle–Upper Jurassic shales and carbonates of the Chaman Bid Formation in the western Kope-Dagh (Afshar Harb 1979; Mahboubi et al. 2001); and Bajocian to Bathonian mudstones of the Kashafrud Formation may also have generated hydrocarbons in the eastern Kopet-Dagh (Poursoltani et al. 2007, Poursoltani and Gibling 2011; Sardar Abadi et al. 2014) (Fig 1). The objectives of this study are facies analysis, recognition of diagenetic history and estimation of porosity of the Mozduran Formation in Mazdavand area.

*Corresponding author.

E-mail address (es): poursoltani1852@mshdiau.ac.ir

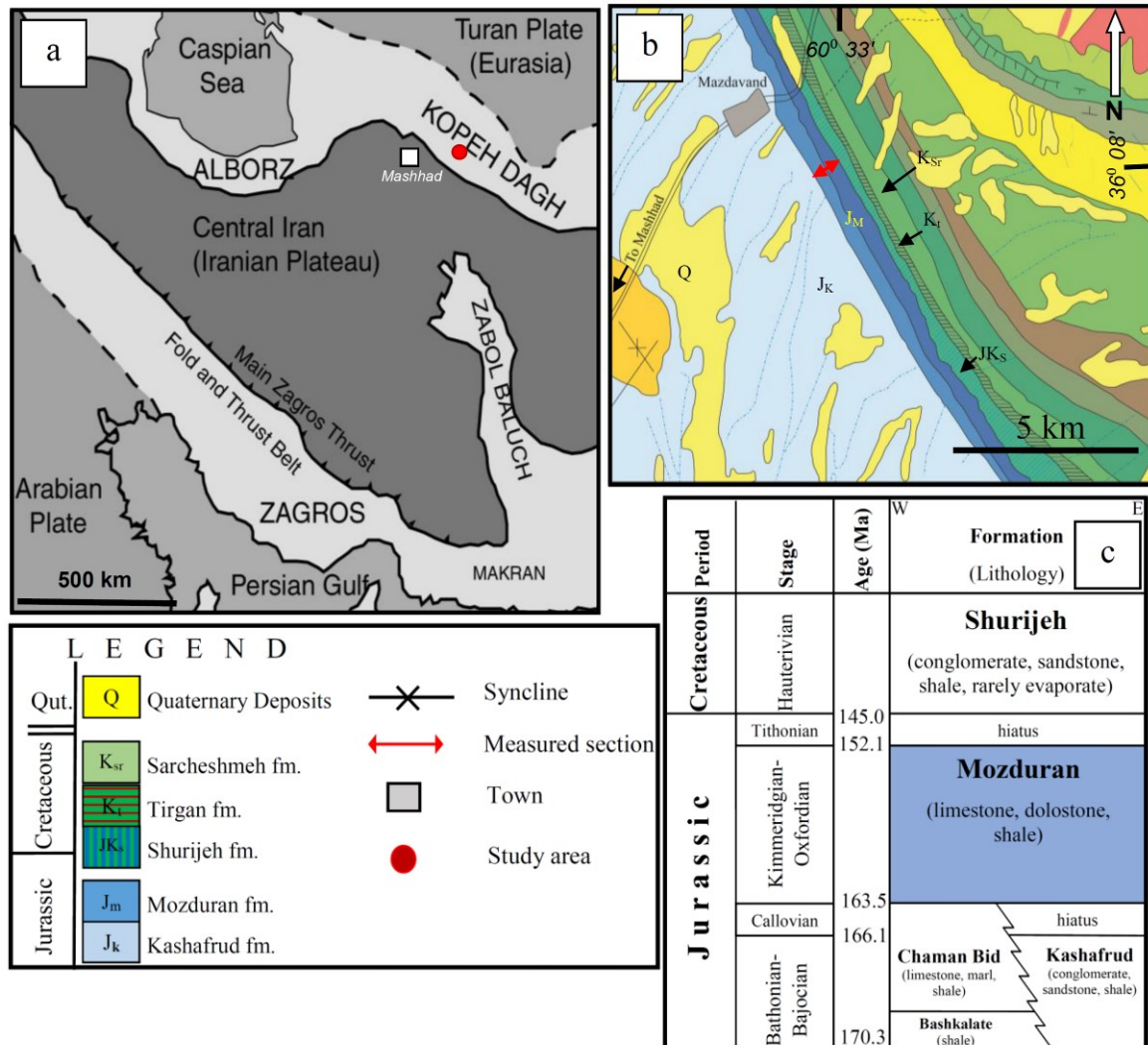


Fig 1. a) Location map of Iran and study area in the Kopet-Dagh Basin of northeast Iran. Modified from Geological Survey of Iran, www.gsi.ir. b) Geological map shows the location of the studied section (arrow), simplified from Iran Geological Survey map sheet Mozduran-Shir Tappeh (1:100,000 scale). c) Generalized Upper Jurassic and Lower Cretaceous stratigraphy of the studied formation, at the Mazdavand area (not to scale). Approximate ages for the formations are based on biostratigraphic studies (Aghanabati 2004), linked to the timescale of Gradstein et al. (2012).

2. Stratigraphy and Geological setting

Kopet-Dagh is one of the most important zones in Iran, which extends along the border area between Iran and Turkmenistan, is located within the Alpine-Himalayan orogenic belt, and is defined as the northern limit of the Cenozoic deformation in Iran (Hollingsworth et al. 2006).

The Kopet-Dagh Basin, together with the Amu-Darya Basin to the south in Turkmenistan, form a large intracontinental basin filled by a thick post-Triassic sequence of mostly marine sediments that mainly consist of limestones, marls and sandstones (Stöcklin 1968; Berberian 1976). These sedimentary sequences record an almost complete succession from Lower Jurassic to Pliocene rocks (Lyberis and Manby 1999). Less is known about the deformation history of the pre-

Jurassic successions in the Kopet-Dagh, although it has been interpreted as resulting from the closure of the Paleo-Tethys (Afshar Harb 1979; Poursoltani et al. 2007). The successions are partly eroded by and unconformably overlain by Jurassic and younger sediments (Afshar Harb 1979). The opening of the Kopet-Dagh-Amu-Darya Basin started in the early Jurassic. Subsidence was mostly linked to major E-W trending normal faults. This continuous subsidence led to the deposition of the thick post-Triassic sequence of mostly marine sedimentary rocks. Onset of the convergence between the Iran and Turan blocks started in the Paleocene and gave rise to the inversion of the basin (Bretis et al. 2012). A relatively high subsidence rate of 98.2 m per million years was calculated for the eastern Kopet-Dagh by Moussavi Harami and Brenner (1992).

During the Callovian, a marine transgression from the northwest resulted in the deposition of the Mozduran carbonates, which disconformably overlie the marine siliciclastics of the Kashafrud Formation and are capped by red siliciclastic rocks of the Shurijeh Formation, which were deposited by fluvial depositional systems, in

the eastern Kopet-Dagh area (Lasemi 1995). The upper contact of the Mozduran Formation with the red continental deposits of the Lower Cretaceous Shurijeh Formation is marked by an erosional unconformity in most places (Figs 1c - 2).

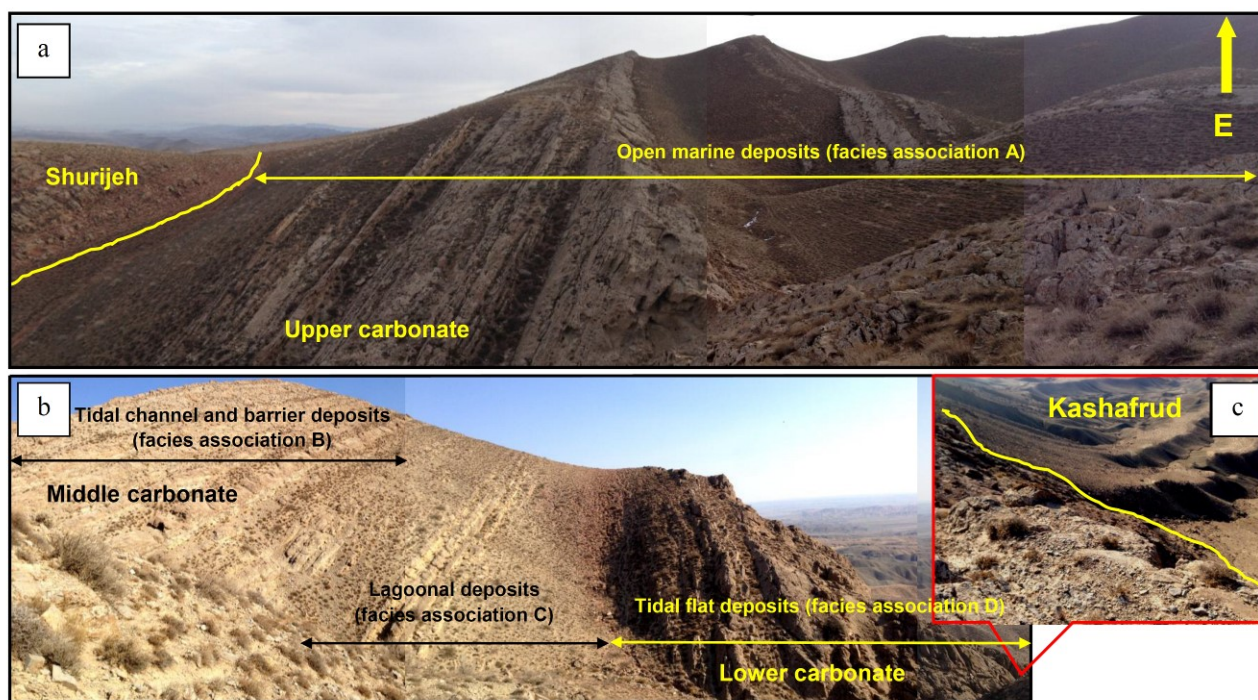


Fig 2. Panorama of Mozduran Formation in the Mazdavand area. Lower and upper contact with older and younger formations (Kashafrud and Shurijeh) is marked.

From Mazdavand eastwards, the thickness of the Mozduran Formation decreases and gradually changes to nearshore, mainly siliciclastic deposits in eastern Kopet Dagh (Afshar Harb, 1979, Zand Moghadam et al., 2014). This formation at the type locality, Mozduran area, is mainly composed of limestone, dolostone and less amounts of shale interbeds, ranging in thickness from 420 to 1380 m at the type section and Khangiran well #31, respectively (Afshar-Harb 1994).

In study area, three informal carbonate units were recognized (Figs 2-3). The lower carbonate, 92 m thick, consists predominantly of massive to thick bedded yellow to gray dolomudstone to sandy dolostone, interbedded with grainstone and packstone. The middle carbonate, 125 m thick, consists massive, medium to thin bedded wackstone, packstone, shale and yellow dolomudstone. The upper carbonate, 30 m thick, consists thin to thick bedded wackstone and yellow dolomudstone.

3. Methods

In this study, one outcrop section from the Mozduran Formation (Mazdavand area) (Fig 1b), was measured bed-by-bed, and samples were taken systematically for a total of 470 m, and facies types were identified. Over

250 fresh carbonate samples were collected, from which 115 thin sections were made (Fig 3). Carbonates were classified using the Dunham (1962) scheme. The grains and matrix percentages were estimated using visual percentage charts (Flügel 1982, 2010). Field observations were used to assess the lateral extent and thickness variation of carbonate and mudstone. Facies types and depositional settings were interpreted based on compositional, textural, fabric, and sedimentary data (e.g., Purser 1969; Wilson 1975; Tucker and Wright 1990; Flügel 2004).

Twenty polished thin sections were analysed using a Nikon Eclipse E400-POL microscope equipped with a Reliotron III cathodoluminescence (CL) system (Relion Industries LLC, Bedford, MA, USA). CL photomicrographs were taken with a beam current between 4.2 and 5.1 KV and under a vacuum of 68.5 to 71.5 m Torr. CL microfabrics provided insight into paragenetic relationships not observed using standard petrographic techniques. Qualitative analysis of textural relationships was used in combination with quantitative data to constrain the diagenetic history. In addition, porosity was estimated from counts of 500 points in each of 115 thin sections prepared separately with blue

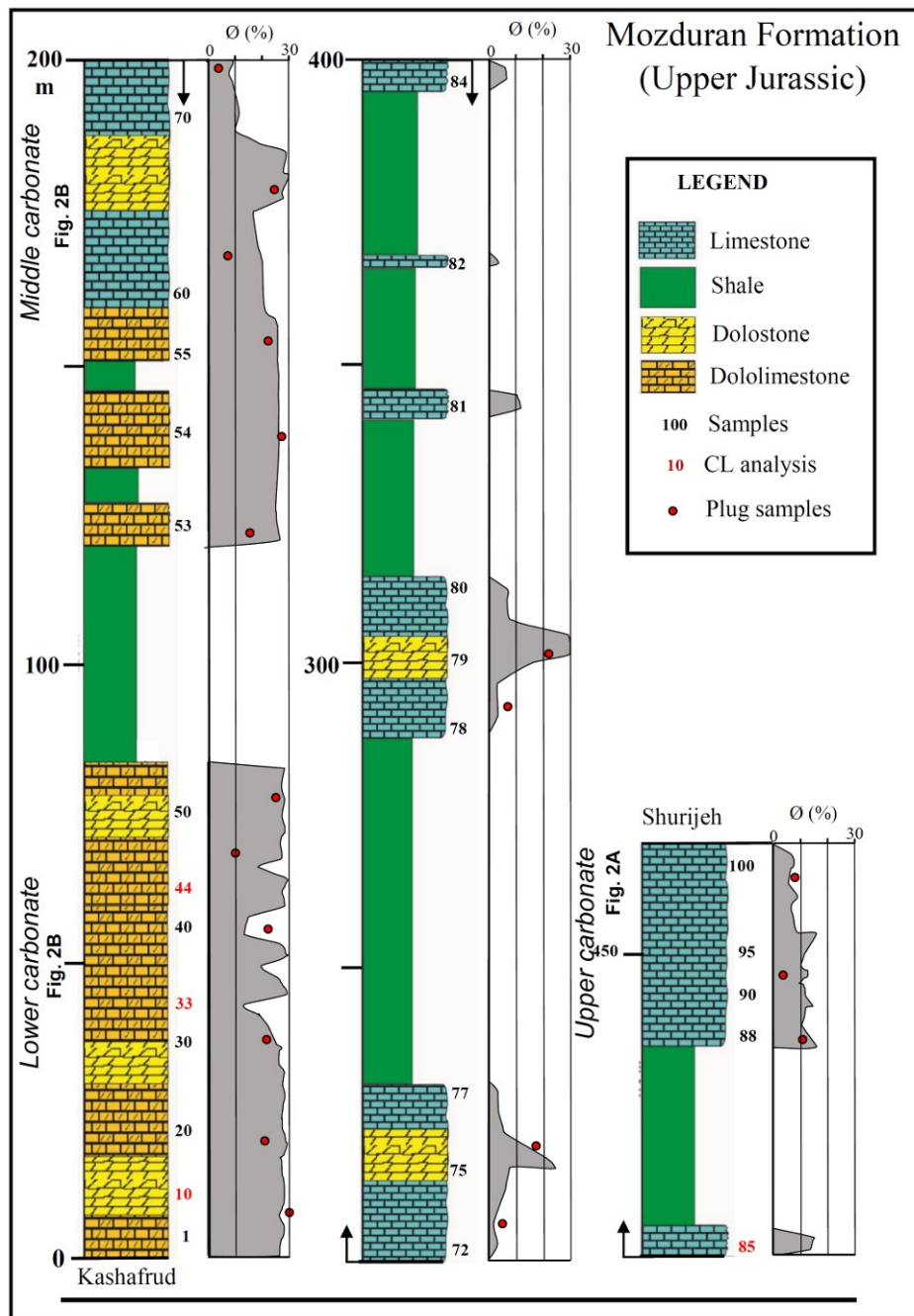


Fig 3. Stratigraphic log for the Mozduran Formation in the study section, showing sample positions. Location of section is shown in figure 1b. Grey curve shows two-dimensional porosity, and red circles show plug samples.

epoxy, each of 115 thin sections prepared separately with blue epoxy, and also were determined on 19 plug samples that cover all carbonate units (Fig 3) using standard procedures at Core Laboratories of National Iranian Oil Co. Helium porosity was measured at ambient temperature and pressure. Three carbon-coated polished thin sections were studied to determine the composition and imaging using a LEO 1450 VP at an acceleration voltage of 30 kV, equipped with an Oxford 80 mm² SDD-EDS detector and INCA software.

4. Facies and depositional environment

Field and petrographic studies of the Mozduran Formation led to the recognition of several vertically stacked lithofacies grouped into four carbonate facies associations at the Mazdavand outcrop. The lithofacies recognized and their interpretations are shown in Table 1.

4.1. Open marine deposits (facies association A)

Bioclasts included pellet, echinoid, brachiopod, bryozoan, bivalve, red algal and gastropod fragments, and non-skeletal grains consist of intraclasts, ooids and

fine-grained quartz. These facies are mainly mudstone (bioclastic mudstone, mudstone, sandy bioclastic mudstone), wackestone (peloidal bioclastic wackestone, intraclastic bioclast wackestone, bioclastic wackestone), packstone (bioclastic ooid packstone, intralastic ooid packstone, intraclastic bioclast packstone and sandy bioclastic packstone), and dark grey and massive marl/shale (Fig 4a, b, c).

4.1.1. Interpretation

The open marine is suggested by the presence of a facies association of bioclastic wackestone with dark grey marl/shale, and also by the abundant and diversity of shelled organisms. The carbonates of the thin-bedded basinal limestone and the ooids, intraclasts, bioclasts and fine-grained quartz could have been deposited as debris, shed off the adjacent platform margin (e.g., Lasemi 1995; Sanders and Hofling 2000; Flugel 2004; Mahboubi et al. 2010).

4.2. Tidal channel and barrier deposits (facies association B)

These facies are composed of peloid ooid grainstone/packstone, bioclastic ooid grainstone/packstone, bioclastic intraclast grainstone

and ooid bioclastic grainstone (Fig 4d). Ooids, pellets and intraclasts are the main non-skeletal grains of this facies association. Planar and trough cross-bedding are the main structures.

4.2.1. Interpretation

The abundance of oolitic cross-bedded grainstone, the scarcity of mud and the well-sorted nature of this facies association indicate a high-energy condition, probably where tidal channels or inlets cross a barrier which, separating the open-marine environment from a more restricted lagoonal area (e.g. Coffey and Read 2004). Cross-bedding probably resulted from sand-wave migration. The abundance of intraclasts indicates rip up and erosion of the previous deposits by storms or tidal channels (Lasemi 1995).

4.3. Lagoonal deposits (facies association C)

Mudstone, wackestone (bioclastic wackestone, peloid bioclastic wackestone, bioturbated mudstone/wackestone, sandy bioclastic wackestone), packstone/wackestone (bioclastic peloid packstone/wackestone), packstone (bioclastic intraclast packstone, peloid intraclast packstone, peloid oncoid packstone), and dolostone (bioclastic dolomudstone, oncoied dolomudstone) (Fig 4e). Bioclasts are mostly ostracods, and quartz and oncoids are the main non-skeletal fragments.

Table 1. Summary of characteristics and interpretation of lithofacies of Mozduran Formation in the study area.

Facies association	Rock name	Sedimentary features	Depositional condition
A	mudstone wackestone packstone marl/shale	Bioclasts included echinoid, brachiopod, bryozoans, bivalves, red algae and gastropod, whereas, are non-skeletal grains consist intraclast, ooid and fine grain quartz.	The open marine is suggested by presence of facies association bioclastic wackestone, and dark grey marl/shale.
B	grainstone packstone	Ooid, pellet and intraclasts are the main non-skeletal grains of this facies association. Planar and trough cross-bedding are the main structures.	The abundance of oolitic cross-bedded grainstone and the mud free indicate a high-energy condition such as barrier, and also the existence of intraclasts indicates erosion of the previous deposits by storms or tidal channels.
C	mudstone wackestone packstone dolostone	Bioclasts include mostly ostracod, and pellet and quartz is the main non-skeletal fragments.	The lagoonal and shallow subtidal environments are suggested by presence of bioturbated and pelleted lime mudstone/ wackestone within the mud-supported and also the peloid intraclast packstone, and peloid oncoid packstone.
D	mudstone dolostone	Thin to medium bedding, laminated lime mudstone and mud-crack are the main structures.	The presence of thin-bedded dolomudstone and fenestral pellet lime mudstone/ wackestone, and mudcrack is interpreted the supratidal environment.

4.3.1. Interpretation

The presence of bioturbated and pelleted lime mudstone/ wackestone within mud-supported strata indicates a low-energy lagoonal environment, whereas the peloid intraclast packstone and peloid oncoid packstone suggest higher-energy conditions in a shallow subtidal setting (landward or seaward side of the lagoon) (e.g. Lasemi 1995; Alsharhan and Kendall 2003).

4.4. Tidal flat deposits (facies association D)

These facies are mainly mudstone (fenestral pellet lime mudstone/wackestone) and dolostone (dolomicrite, sandy dolostone, dolostone, sandy coarse-grained dolostone). Thin to medium bedding, laminated lime

mudstone and mud-cracks are the main structures (Fig 4f).

4.4.1. Interpretation

Thin-bedded dolomudstone and fenestral pellet lime mudstone/ wackestone, and also subaerial exposure features such as mud-cracks are interpreted to represent deposition in a supratidal environment (e.g., Lasemi 1995; Alsharhan and Kendall 2003; Warren 2006; Mahboubi et al. 2010). These characteristics indicate deposition on tidal flats, similar to those of carbonate tidal flats of Persian Gulf (Shinn 1986; Chafetz et al. 1999).

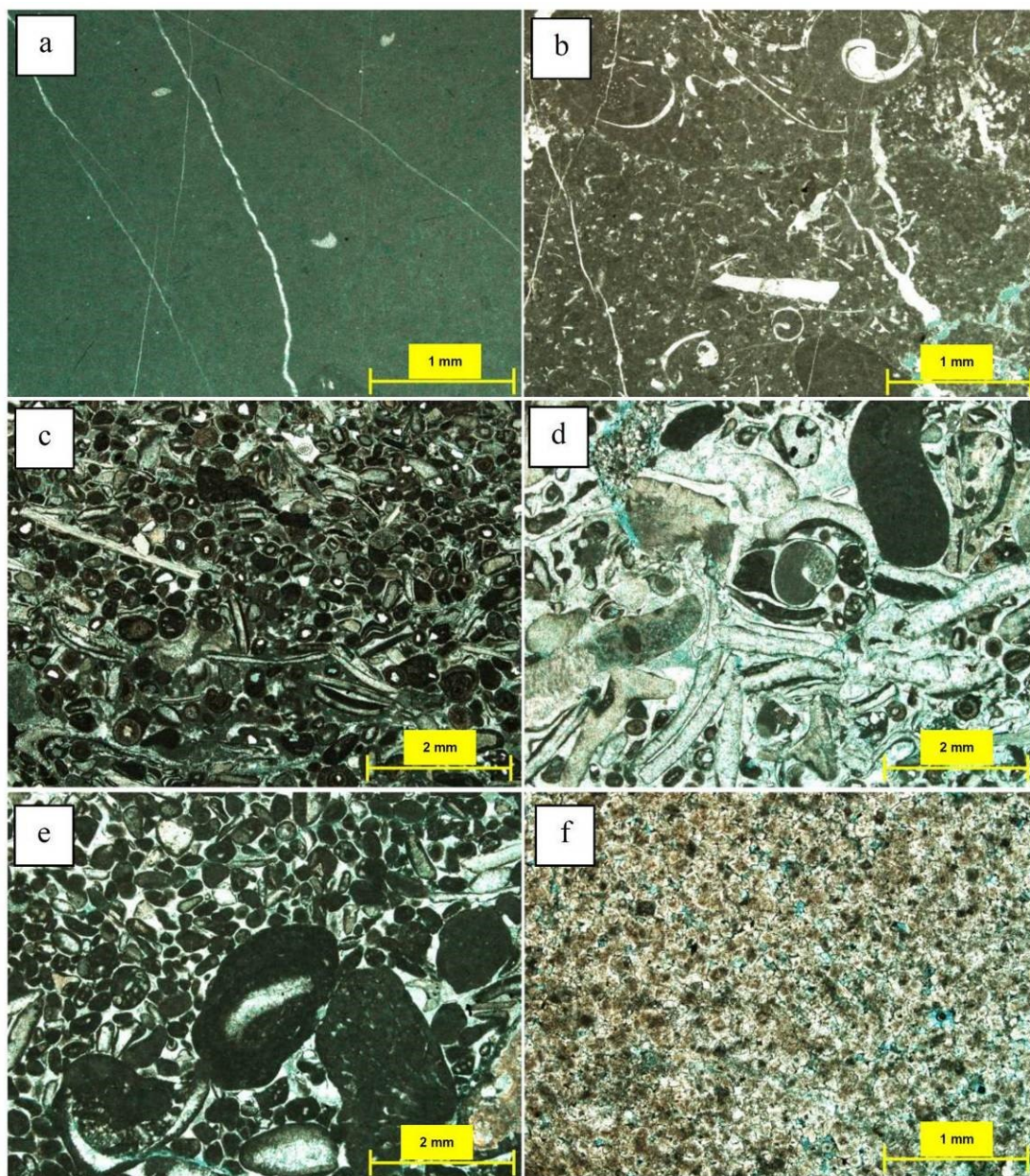


Fig 4. Thin section photomicrographs of samples of the study area. a) Mudstone (64); b) Bioclastic wackestone (73); c) Intraclastic bioclastic ooid packstone (90); d) Ooid bioclastic grainstone (D); e) Peloid intraclast packstone (81); f) Dolostone (12) (a-c: facies association A; d: facies association B; e: facies association C; f: facies association D).

4.5. Depositional model

Our studies indicate that, in the study area, the carbonates of the Mozduran Formation (carbonate platform) pass into the Kashafrud Formation (fluvial-deltaic to deeper-marine basin (see Geological setting), (Poursoltani et al. 2007; Taheri et al. 2009), and deposited on a rimmed carbonate platform (c.f. Read, 1982, 1985; Tucker and Wright, 1990) is inferred, passing into a carbonate ramp during the late Kimmeridgian (Kavoosi et al., 2009).

Based on our field and laboratory studies, the basal

environment was characterized by dark grey marl/shale formed in an open-marine setting, and most of the carbonate rocks were deposited in a shoal, shelf lagoon, and tidal flat setting (c.f. Read 1985; Tucker and Wright 1990). A depositional model can therefore be defined for the Mozduran strata during the Oxfordian-Kimmeridgian for the study succession (Fig 5). Facies interpretations for the Mozduran Formation have included tidal flat, lagoonal, barrier and open marine. Our study area, three informal carbonate units was recognized (Figs 2-3).

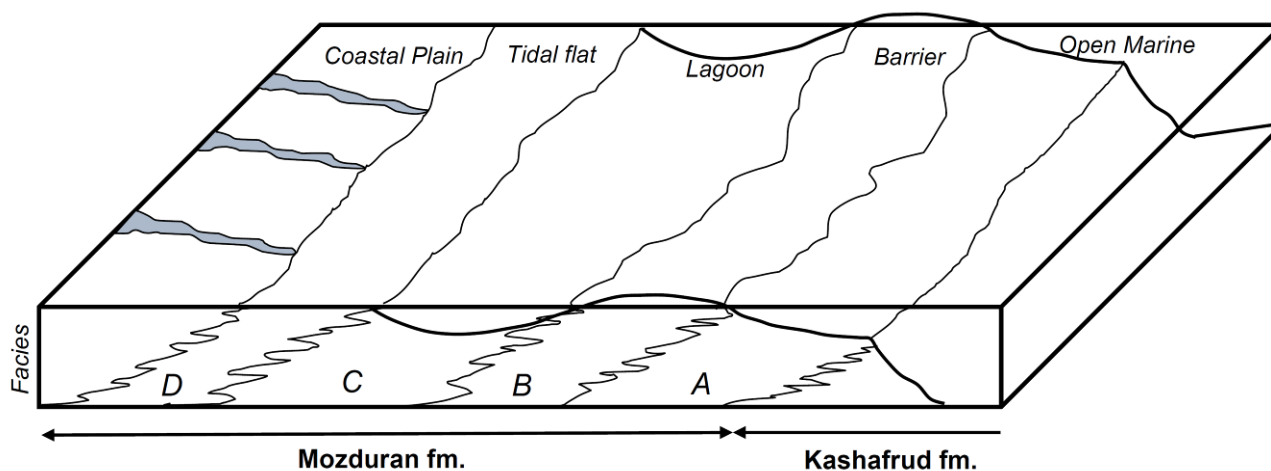


Fig. 5. Diagrammatic illustration of the setting of the Mozduran Formation in the Kopet-Dagh Basin. Progradation phase with the deposition of Mozduran deposits above the marine siliciclastics of the Kashafrud Formation in the eastern Kopet Dagh Basin.

5. Diagenetic events

The Mozduran Formation rocks contain evidence for numerous diagenetic processes, including micritization, cementation, compaction (physical and chemical), fracturing, dissolution, neomorphism, silicification and dolomitization that will be explained and interpreted.

5.1. Diagenetic features in limestones

5.1.1. Cementation

The most important cements are bladed, mosaic, syntaxial overgrowth, blocky and granular, with lesser proportions of iron oxide. For 100 samples, the percentage of cement varies from 2% to 39%, averaging 16.7% (Fig 6).

Granular cement

This type of cement formed as the first generation cement around grains in grainstones. Granular cements reflect high saturation state of CaCO_3 and low sedimentation rate during its formation (Ehrenberg et al. 2002). This type of cement constitutes up to 14% of total cement (Fig 7a).

Bladed cement

This cement exhibits a bladed texture and isopachous fabric with 20–100 μm -long, prismatic crystals (Fig 7b), and is commonly pore filling. Bladed cement is found exclusively in veins and dissolved skeletal grains with pore spaces, as well as on grain rims, and constitutes less than 12% of the total cement volume (Fig 3). It did not significantly affect the petrophysical properties of the limestone.

Mosaic cement (equant)

This is a common cement (39% of the total cement volume), and filled the pores between skeletal and non-skeletal grains and also formed within veins. This cement also formed as subhedral crystals with average size ranging up to 0.15 mm (Fig 7c).

Syntaxial overgrowth cement

Syntaxial overgrowth cement was precipitated exclusively around echinoderm fragments lacking micrite envelopes, and is commonly clear and lacks

inclusions (Fig 7d). This cement constitutes less than 2% of the total cement volume.

Blocky cement

Blocky cement is abundant, and formed in mud-free, grain-supported grainstone lithofacies comprising single crystals with 0.1–0.3 mm diameter. They generally occupy the remains of pores (Fig 7e). This type is a major cement, as a second generation, and constitutes up to 31% of total cement.

Iron oxide

Iron oxide is a minor type of cement and forms less than 2% of cement volume on average. The oxides commonly fill pores and narrow intergranular spaces (Fig 7f, g).

5.1.2. Silicification

In a few beds, silicification is found mainly in limestone interbedded with thin shale beds. Silica replacements (chalcedony or micro-quartz) occur within bivalve and brachiopod shells (Fig 8a). The main type of silicification is fabric selective.

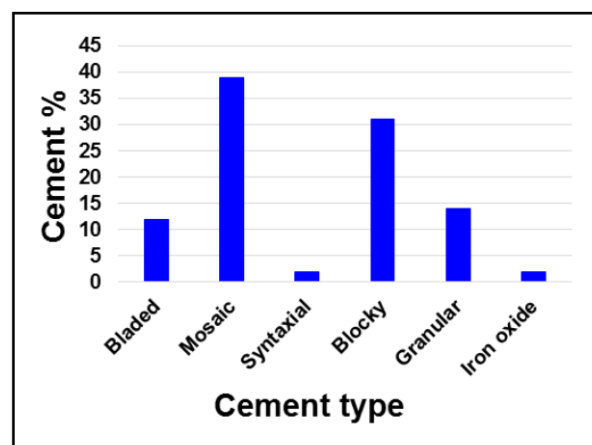


Fig 6. Histogram of cement types in study samples. Cementation was determined by point counting thin sections (115 samples).

5.1.3. Neomorphism

Neomorphism is one of the main events that occurred in the studied samples. The replacement of coarser crystals instead of very fine crystals, and also recrystallization, are the result of this event (Folk 1965; Bathurst 1975). The filling of some skeletal and non-skeletal grains (mostly ooids) with sparry calcite formed from metastable aragonite mineralogy. This type is mainly seen in oolitic grainstone, bioclastic grainstone and packstone (Fig 8b). This process in general changed lime mud to coarser crystals in mud-supported facies, such as wackstones and bioclastic mudstones.

5.1.4. Fracturing

As evident from microscopic study, grains contain microfractures. Microfractures are straight traces that cut numerous grains and associated cement, and in some cases formed veins. These veins have been filled with coarse crystalline sparry calcite (Fig 8c). Another type of fracturing occurred on grains due to compaction. Some ooids and shell fragments contain microfractures that were well cemented (Fig 8d).

5.1.5. Compaction and pressure solution

The Mozduran carbonate rocks display considerable compactional effects arrested by cementation in some beds. Compaction led to physical and chemical rearrangements and changes in the sediments. Physical compaction caused close packing, close grain contacts and also decrease of primary interparticle porosity in grain-supported limestones (Fig 8e). Some ductile grains (such as intraclasts) are bent around resistant detrital grains, and ductile mud clasts have locally been deformed sufficiently to produce pseudomatrix, thus decreasing porosity.

Skeletal (brachiopods, bivalves and echinoderms) and non-skeletal grains (ooids) have been intensively fractured during mechanical compaction. Additionally, during burial chemical compaction started and changed some of the sediment characteristics. Grain contacts are predominantly concavo-convex and sutured, with subordinate point contacts. Where grains are closely packed, there is indication of some degree of intergranular pressure solution and the formation of stylolites (Fig 8e).

5.1.6. Micritization

Micritization is common in the Mozduran carbonates (Fig 9a). This process is generated by repetition of microorganism activities involving bacteria and algae on carbonate grain surfaces (Carols 2002). Micrite envelopes (5 to 35 μm thick) mostly developed around bioclasts such as bivalve and brachiopod shells, as well as on non-skeletal particles such as peloids, ooids and intraclasts. They are attributed to micro-borer organisms living at or near the sediment-water interface (Tucker and Wright 1990; Vincent et al. 2007; Brigaud et al. 2009).

5.1.7. Dissolution

Evidence of dissolution is present in most samples in the study section. In many samples, grains, matrix and

carbonate cement all show partial dissolution (Fig 9), and a few oversized pores suggest complete dissolution of some grains. Moldic dissolution of the skeletal (mostly gastropods) and non-skeletal (mostly ooid) grains was pervasive in the study sections. The moldic voids are progressively filled with blocky cements, suggesting a very early process (e.g. Brigaud et al. 2009). Secondary porosity was generated by dissolution of grains and cement in many samples.

5.1.8. Dolomitization

Dolomitization is the most important process in the Mozduran carbonate rocks, in the studied samples. Based on petrographic evidence (e.g., Sibley and Greeg classification 1987), dolomites in the study area have been divided into four types.

1- Very fine crystals (D1): This type shows fine crystals with anhedral and rarely subhedral shape and the size is more than 50 μm . In some samples, allochems show dolomitization. In studied samples sparse detrital quartz grains are observed (Fig 10a).

2- Medium and euhedral crystals (D2): Type two (D2) shows medium crystals with euhedral shape and the size is up to 150 μm . This type is fluted in the mudstone (Fig 10b). In studied samples the replacement of matrix has occurred, but some of allochems show this process in wackestone (Fig 10c). In some carbonate grains of grainstones, replacement is observed. Most of the samples seem to be a dolomudstone that is variably recrystallized. The study samples shown in Figures 11A and 11B show burial dolomite rhombs (based on very dull luminescence) and what might be secondary solution enhancement (brighter areas). It is also suspected that like many producing dolostones, intercrystalline porosity is important. In some cases more than one generation of dolomite is visible (Fig 11b, c). The euhedral dolomite rhombs with cloudy cores and limpid (clear) rims resemble sucrosic dolomite.

3- Coarse and euhedral crystals, with zoning (D3): Type three shows coarse crystals, mostly euhedral crystals to subhedral shape. Their size is more than 250 μm (Fig 10d). This type is locally porefilling. These dolomites have cloudy centers and clear rims. The lack of calcite inclusions makes for bright and clear outer parts of the crystals. This type can be generated from different fluids (Kyser et al. 2002; e.g. Mahboubi et al. 2010).

4- Coarse and euhedral and anhedral crystals, pore-filling (D4): The size of crystals is more than 300 μm . Generally, this type fills the pores and fractures (Figs 10e and 11e, f). Some dolomite rhombs are discernible. In rare instances, a slightly brighter blocky cement fills what looks like secondary porosity. This might suggest meteoric precipitation upon uplift. As Sibley and Greeg (1987) discussed, different crystal size types of dolomites can be accounted for by the relationship between nucleation and kinetic growth as well as relative timing. Increasing the temperature causes the rate of nucleation and crystal growth to increase.

6. Discussion

6.1. Paragenetic sequence

A paragenetic sequence for the Mozduran Formation is set out in figure 12. In carbonate systems, grain size and texture, mineralogy, nature of pore fluid, climate, and sediment type affect the sequence of diagenetic events (Tucker and Wright 1990; Tucker 1993; Flugel 2004).

The study area deposits show different stages of diagenesis, including eodiagenetic, mesodiagenetic and telodiagenetic states. Eodiagenetic involves marine, meteoric and mixing zone environments. Most of the processes occurred in meteoric and burial environments. The main diagenetic events are distinguished as predating or post-dating.... predating or postdating what?

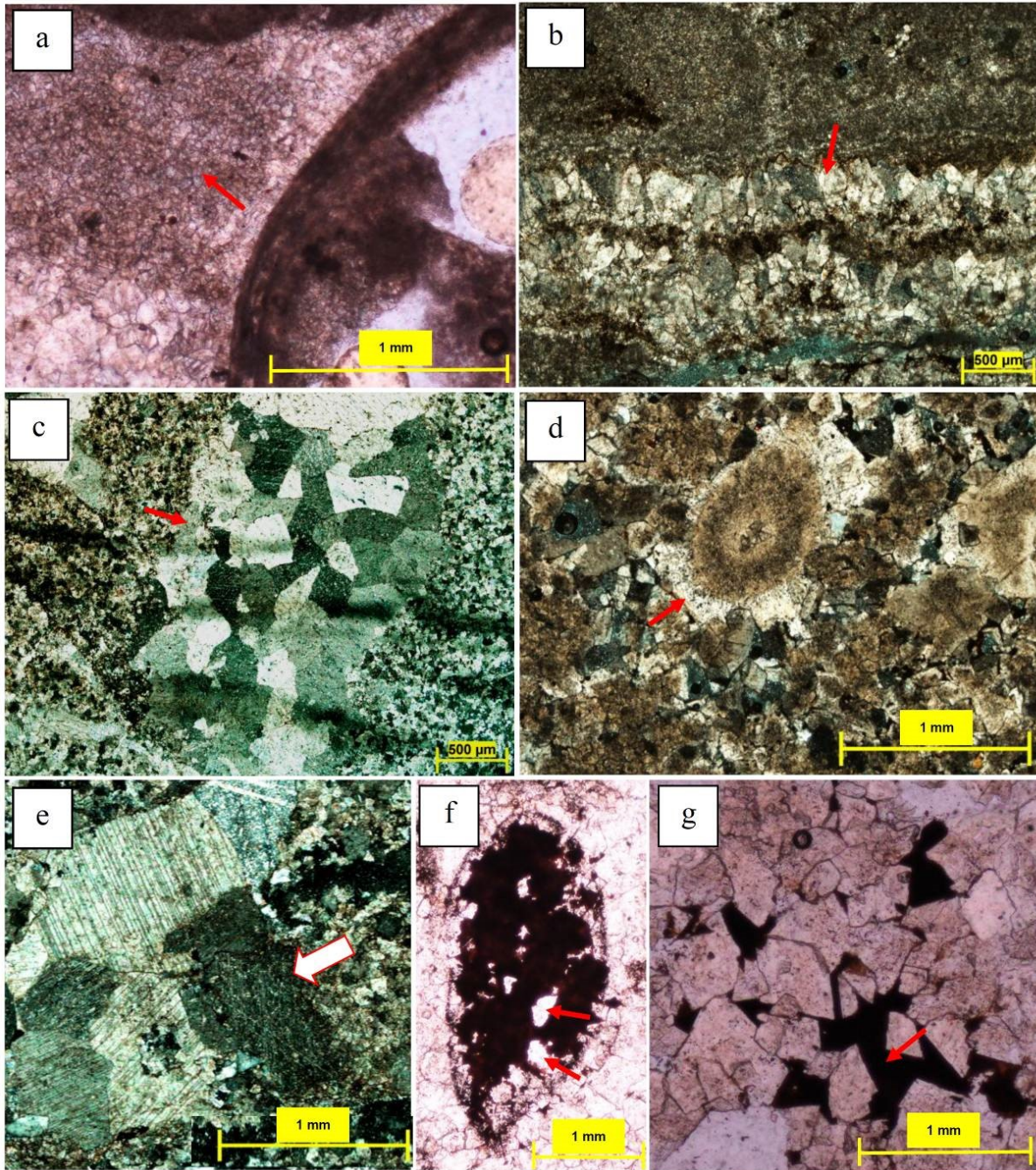


Fig 7. Thin section photomicrographs of samples to show the effect of diagenetic processes. a) Granular cement in grainstone (88); b) Bladed cement which filled a vein (38); c) Mosaic cement that formed as subhedral crystals, filling pores (36); d) Syntaxial cement precipitated around echinoderm fragments (16); e) Coarse crystalline blocky calcite that occupies the pores (1); f) Iron Oxide filling a moldic pore. A few remained pores are observed (arrows) (5); g) Iron Oxide cements filling pores in dolostone, with euhedral dolomite crystals observed (41).

Based on petrographic results, micritization, cementation, compaction (physical and chemical), fracturing, dissolution, neomorphism, silicification,

iron-oxide cementation, and dolomitization are the main phases of diagenetic events, and have operated in three different environments (Figs 11 and 12).

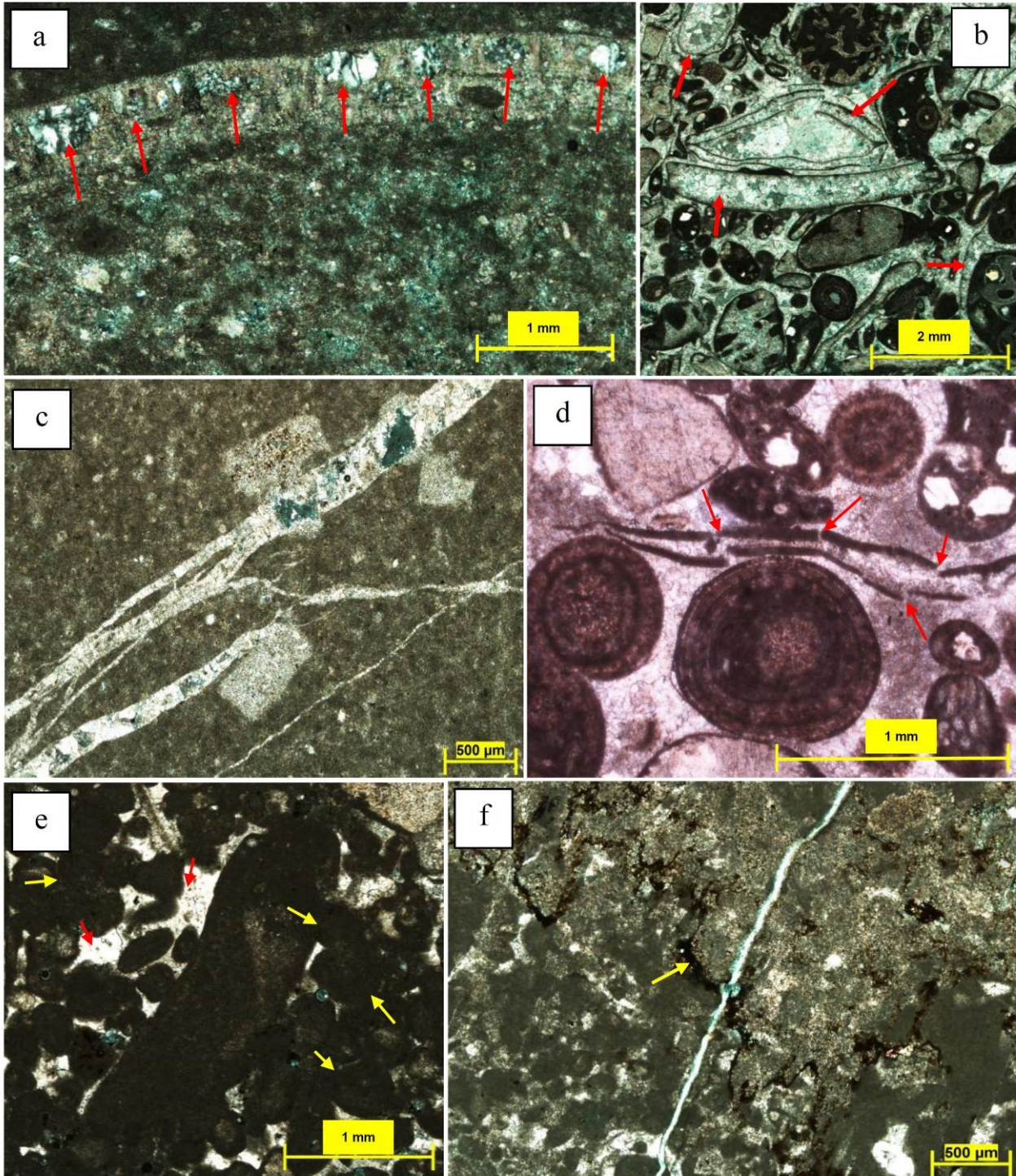


Fig 8. Thin section photomicrographs of samples to show the effect of diagenetic processes. a) Silica within brachiopod shells (arrows) in a wackestone (82); b) Neomorphism in skeletal shells in grainstone (arrows) (91); c) Fractures in mudstones filled by calcite cement (45); d) Grain fracturing (arrows) (89); e) Compaction in a packstone, yellow arrows show grain contacts, the pores filled by sparite (red arrows), probably before compaction (29); f) Stylolite in wackestone, filled with Iron Oxide (38).

Eodiagenetic stage

In the Mozduran Formation, early diagenetic stage is recognized by micritization, physical compaction, dissolution, calcite cementation (blocky, bladed, mosaic, granular), Fe-oxide, neomorphism and dolomitization, which covers the point of deposition to shallow burial below the depth of marine, meteoric phreatic and mixing zone environments (e.g., Vincent et al. 2007). Mechanical compaction, resulting in disaggregation of rock fragments and deformation of soft grains, may have commenced immediately after burial

(see Götte et al. 2013), continuing through deep burial (Dickinson and Milliken 1995).

Palmer et al. (1988) and Ferry et al. (2007) suggested that, in a calcite-sea context, such early dissolution of aragonite might have occurred either in seawater or under very shallow burial conditions, but it might also have occurred during deep burial. A probable factor could be penetration of undersaturated water, near the surface, that might have led to dissolution.

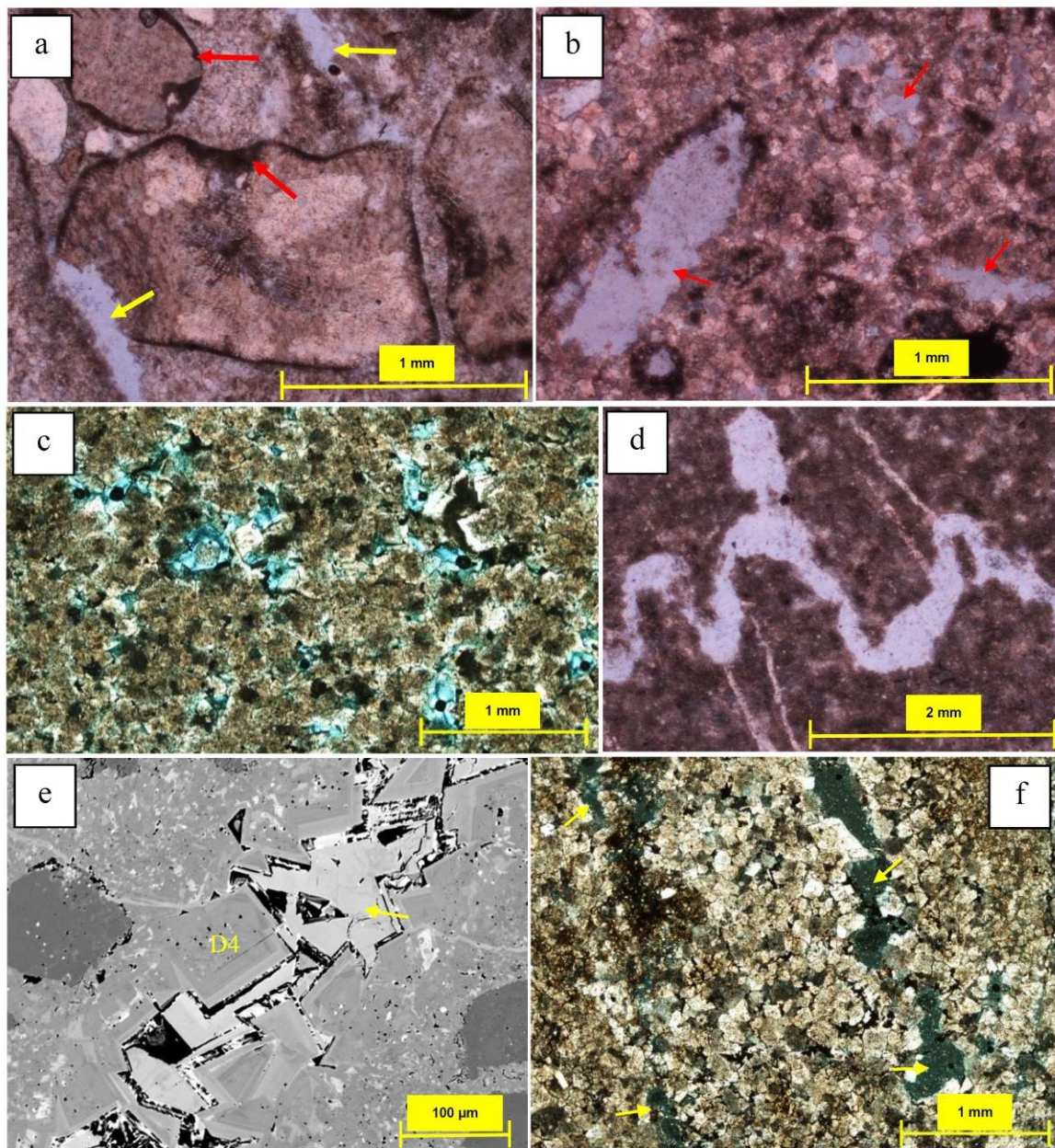


Fig 9. Thin section photomicrographs of samples of the study area. Porosity is filled with blue epoxy. a) Micritization that affected the fragment margins in a packstone (red arrows); yellow arrows show dissolution of cements and some part of grains (88); b) Dissolution of the grains (fossil fragments), forming interparticle porosity (arrows) (5); c) Intercrystalline porosity in dolostone (6); d) Stylolite type porosity (78); e) Back-scatter electron micrograph, showing dissolution in dolostone that formed a vuggy porosity (D4) (7); f) Channel type porosity in dolostone (arrows) (17).

Mesodiagenetic stage

Greater depth and higher temperature affected the Mozduran Formation in this diagenetic stage. Burial diagenesis of the Mozduran rocks was dominated by some main processes: cementation (mosaic, syntaxial, blocky), silicification, dissolution, physical and chemical compaction (stylolites, increasing grain contacts), grain fracturing, neomorphism, dolomitization and rarely Fe-oxide cementation. Textural evidence suggests a close relationship between replacement of subhedral to euhedral dolomites. Silicification commenced early and continued through much of the burial history.

The presence of quartz veins in formerly open fractures suggests a later phase of silica cementation, possibly associated with tectonic episodes during later burial or exhumation. Temperatures suggested for their formation range from ~55 to 156 °C (Land 1984; Dutton and

Diggs 1990; De Ros 1998; Lander and Walderhaug 1999; Worden and Morad 2000; Schmid et al. 2004). Based on studies by Mussavi-Harami and Brenner (1992), maximum burial depth of Mozduran Formation is calculated at about 4,000 m. Assuming a surface temperature of 25°C and a geothermal gradient of 25°C/km, the temperature at the Mozduran Formation may not have exceeded 150°C. Mahboubi et al. (2010) inferred a temperature from the lightest oxygen isotope value of about 50° C for Mozduran Formation during Late Jurassic to Early Cretaceous time, correlating with a burial depth of 1300 m in that time. In the Mozduran Formation, textural criteria for early mechanical compaction include bending of mud intraclasts, improved grain packing, and fracturing of the brittle grains.

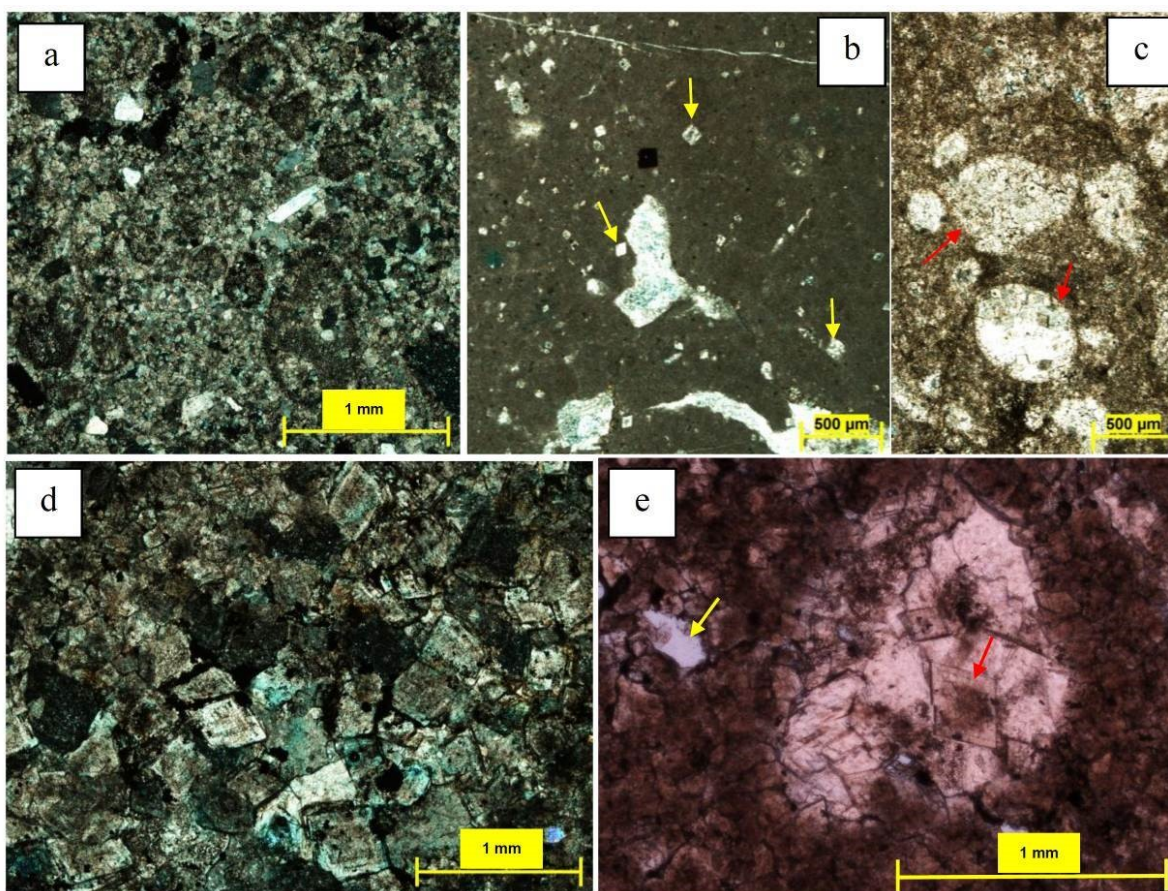


Fig 10. Thin section photomicrographs to show dolomitization as a main diagenetic process in the Mozduran Formation. a) Finely crystalline dolomite (D1 type), dolomitization of allochems and detrital quartz are observed (5); b) Euhehedral shape is fluted in the mudstone (D2 type) (44); c) Dolomitization of allochems in wackestone (D2 type) (33); d) Type three (D3), euhehedral crystals showing zoning (11); e) Euhehedral crystals that fill the pores (D4) (yellow arrow), red arrow showing dissolution (27).

As in formations elsewhere, more broadly the intimate association between secondary fractures, cementation along fractures, and suturing of grains suggests a link between grain deformation, pressure solution and cementation (Milliken 1994; Dickinson and Milliken 1995). Some samples display limited mechanical compaction, probably due to early cementation. Compaction is usually most important during the first 2 km of burial (Worden and Morad 2000).

In some samples, pressure solution of grains may have taken place relatively early in burial, before precipitation of most cements (e.g. Friis et al. 2010). However, as noted below, calcite and dolomite cements show textural relationships that indicate early formation, implying precipitation over a similar burial range to silica cement.

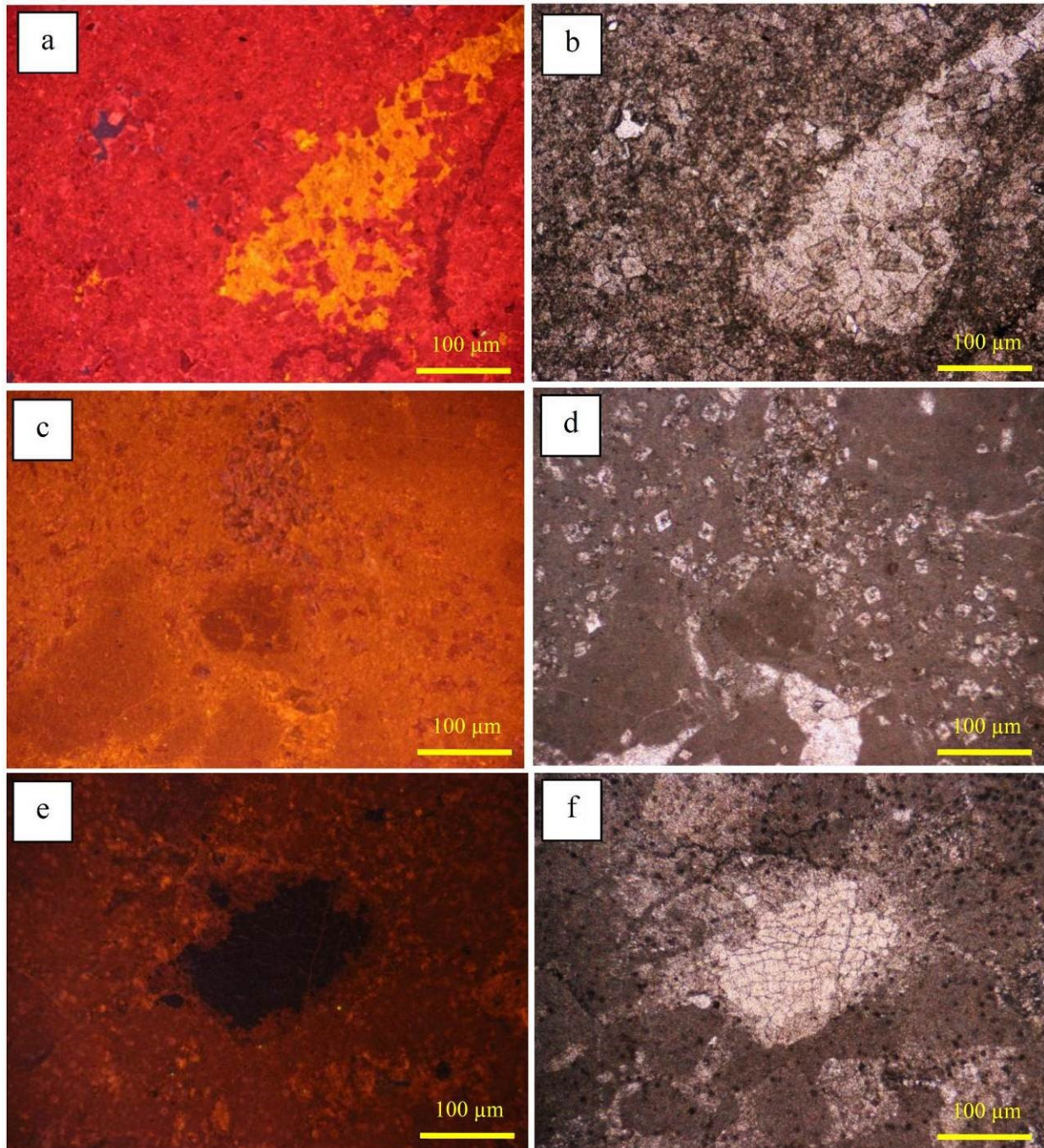


Fig 11. Thin section photomicrographs of samples of the study area under CL. a) Dolomite rhombs and secondary solution (brighter areas) (b the same sample in PPL) (33); c) A dolomudstone that is variably recrystallized (d the same sample in PPL) (44); e) Blocky cement fills pores. Some dolomite rhombs are discernible (f the same sample in PPL) (85).

Time		Eodiagenesis			Mezodiagenesis	Telodiagenesis
Events		Marine	Meteoric	Mixing zone	Burial	Uplift
Cementation	Blocky calcite	-----	-----			
	Syntaxial calcite		-----			
	Bladed calcite	-----				
	Mosaic	-----	-----			
	Granular	-----	-----			
Compaction	Physical	-----	-----			
	Chemical					
Dissolution		-----	-----			
Fe-Oxide		-----	-----			
Micritization		-----	-----			
Neomorphism		-----	-----			
Silicification		-----	-----			
Fracturing		-----	-----			
Vein-filling		-----	-----			
Dolomitization	D1	-----	-----			
	D2	-----	-----			
	D3	-----	-----			
	D4	-----	-----			

Fig 12. Simplified paragenetic sequence of the main diagenetic processes in the Mozduran Formation. Heavy lines represent major diagenetic events, light lines represent minor diagenetic events, and dashed lines represent probable diagenetic events.

The bulk of the mosaic calcite cement probably formed during mesodiagenesis (see Mansurbeg et al. 2008). "Floating-grain textures" suggest an origin prior to much compaction, and non-ferroan calcite is typically the first carbonate phase to form (e.g. Machent et al. 2007). Studies suggest that pore-filling calcite precipitates at modest temperatures, in the 20-70 °C range (Girard et al. 2002; Mahboubi et al. 2010). Higher temperatures (60 to 100 °C) have been suggested for calcite that fills small pores between compacted, tightly packed framework grains (El-ghali 2006; see also Mansurbeg et al. 2008).

Dolomitization is one of the important processes in this burial stage. It affected grainstones, pores and veins, and may have occurred at varied depths. Warren (2006) suggested that, in the absence of baroque dolomites and sulphide mineralization, burial depth may have not been very much.

Coarser dolomitic cements that are more brightly luminescent record later fluid flow, possibly as a

consequence of a second phase of burial diagenesis associated with hydrothermal activity. Most of the samples seem to be a dolomudstone that is variably recrystallized, which might be associated with mixing zone dolomitization.

Some dolomite in the Mozduran rocks fills large pores between loosely packed framework grains and replaces and displaces the host sediments, suggesting early precipitation. However, coarse crystals dolomite mainly replace calcite cement, suggesting deeper burial conditions (e.g. El-ghali, 2006), who suggested dolomite precipitation at 65 °C to 130 °C).

Additionally, some unstable grains such as aragonitic bioclasts have been leached away, during deep burial and chemical compaction (Palmer et al., 1988; Ferry et al., 2007).

Telodiagenetic stage

As the samples are from surface outcrops, telodiagenetic processes may have affected the rocks, especially dissolution under recent meteoric conditions (Giles and

deBoer 1990; Götte et al. 2013). In the Mozduran strata, some fractures and veins have been filled with sparry calcite, dolomite (D4) and iron-oxides. In these strata dissolution of cements may have taken place as strata re-entered modern near-surface environments. Acidic meteoric water is the main factor to cause the fractures and veins formed during the late burial and also late diagenetic stages. However, some of these effects may reflect syndepositional tectonics and exhumation earlier (the late Alpien orogenies in the Miocene), prior to deposition of younger formations (Aghanabati 2004). Some dolomite rhombs are discernible. In rare instances, a slightly brighter blocky cement fills what looks like secondary porosity. This might suggest meteoric precipitation upon uplift. Dissolution of framework grains and cements may have taken place as strata re-entered modern near-surface environments.

7. Porosity

Based on our results for the Mozduran Formation rocks, the type of porosity is mainly secondary porosity, and the main types are interparticle, intraparticle, intercrystalline, and fracture porosity, with minormoldic, shelter, channel, stylolite, and vuggy types (Fig 13). The average porosity of core plugs from 19 samples is 15.78%, with a range from 4% to 29%. These values match well with two-dimensional estimates from thin sections, which average 17.95 %, with range from 2% to 29% (Fig 14, Data Repository Table 1). In contrast to this study, our results for the Mozduran Formation carbonate rocks yielded typical values of porosity (North 1985).

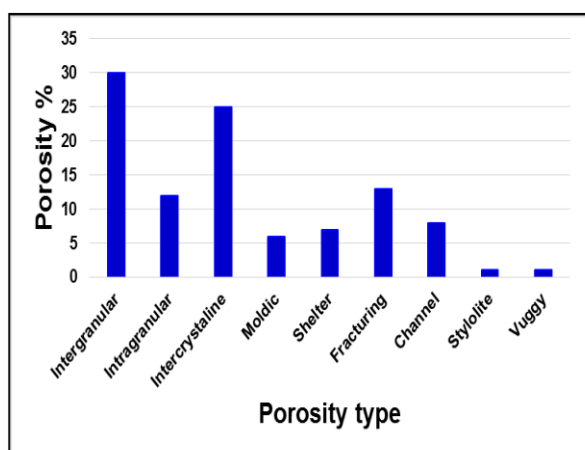


Fig 13. Histogram of porosity types in study samples. Porosity was determined by point counting thin sections stained with blue epoxy (115 samples).

Generally, the highest porosity values occur mostly in dolostone, dololimestone, packstone and grainstone at the lower part, form the bulk of the formation's rocks (Figs 3 and 14), that have been interpreted as tidal channel and barrier and also tidal flat deposits.

Secondary porosity generated by dissolution and fracturing are typically a high proportion of porosity with most pore spaces representing residual primary porosity (Paxton et al. 2002), whereas mechanical and chemical compaction as well as cementation are the primary cause of porosity reduction with increasing burial depth. However, primary porosity appears to have been largely occluded in the low-porosity Mozduran Formation samples, and the small and largely ineffective pores are predominantly secondary.

These more porous samples are either highly fractured or display interparticle and intercrystalline porosity, but some samples contain an unusual abundance of partially dissolved grains and cements (Fig 9). Intergranular pores are the main type of porosity, where carbonate cements have been corroded and become patchy, and parts of these pores could be primary. Additional pore space is provided from intercrystalline micropores, between calcite and dolomite crystals, and from microfractures developed within grains.

Some microfractures and pores have been filled with carbonate and iron oxides (Figs 8c and 9f, g). Fractures form much of the porosity in some samples, and our assessment of porosity percent and type for these surface samples may not be entirely representative of porosity at depth. Scholle and Halley (1985) and Budd (2001) noted that high porosities and microporosities were preserved after passage through the surficial diagenetic environments, which supports the concept that early diagenesis may modify pore systems without having a major effect on total porosity.

8. Conclusion

In the Upper Jurassic limestone of the Eastern Kopet-Dagh Basin, four carbonate facies associations have been recognized. Based on our studies, the basal environment was characterized by dark grey marl/shale formed in an open-marine setting, and most of the carbonate rocks were deposited in a tidal channel and barrier, lagoon and tidal flat setting. The petrographic results indicate that various diagenetic processes affected Mozduran carbonate rocks, including micritization, cementation, compaction (physical and chemical), fracturing, dissolution, neomorphism, silicification, geopetal fabric and dolomitization. These processes occurred in three diagenetic stages, early, burial and late, with the early stage involving marine and meteoric environments.

Porosity was largely occluded by pore-filling cements of carbonate, iron oxides, and rarely silica. Additionally, compaction during early burial improved packing, fractured grains, and caused pressure solution. In addition, porosity is largely secondary, resulting from dissolution of grains and cements, with some fracture porosity. Some fractures, iron oxide cements, and dissolution may reflect Cenozoic tectonism and uplift that created the Kopet-Dagh mountains.

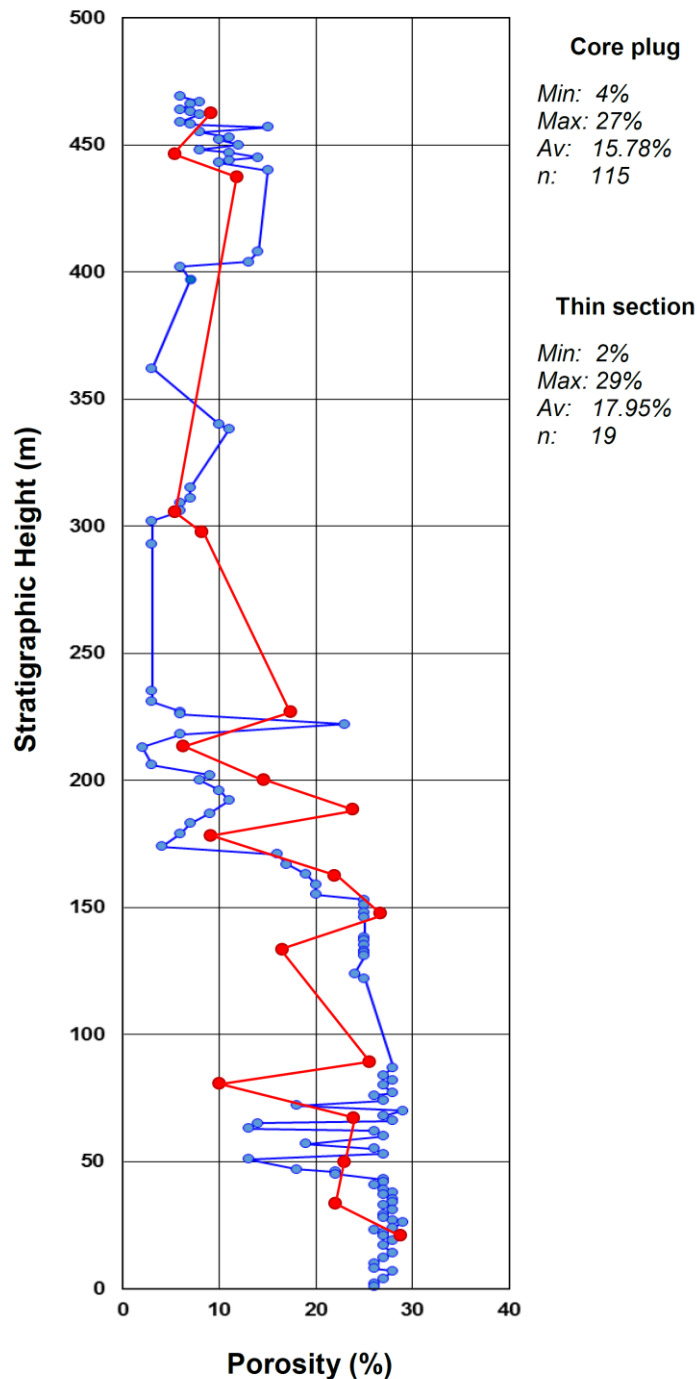


Fig 14. The Comparison of thin section porosity values (blue points) with core plug samples (red points). These values match well with each other.

Porosity analysis of hand samples yields average values for porosity of 17.94%, match well with core plug samples, average 15.78%. Based on the result of this study, the Mozduran Formation carbonate rocks yielded typical values of porosity. The Mozduran Formation results indicate that the search for Upper Jurassic carbonate reservoirs and hydrocarbon systems in the region can be used in the other parts of this basin as well as in similar basins in other parts of the world.

9. Acknowledgements

The authors thank the Islamic Azad University, Mashhad Branch of Iran for financial assistance. We are grateful to Prof. Peir K. Pufahl of Acadia University for CL analysis and his helpful comments, and also would like to thank to Prof. Martin R. Gibling of Dalhousie University for reading an earlier draft of the manuscript, and anonymous reviewers for comments on an earlier manuscript version.

References

- Afshar-Harb A (1979) The Stratigraphy, Tectonics and Petroleum Geology of the Kopet Dagh Region, Northern Iran. Ph.D thesis, Imperial College of Science and Technology, London.
- Aghanabati A (2004) Geology of Iran. Geological Survey of Iran, 586 pp. (in Persian).
- Alavi M, Vaziri H, Seyed-Emami K, Lasemi Y (1997) The Triassic and associated rocks of the Aghdarband areas in central and northeastern Iran as remnant of the southern Turanian active continental margin, *Geology Society of America Bulletin* 109: 1563-1575.
- Allen B, Vincent ST, Alsop GI, Ismail-Zadeh A, Fleckerd R (2003) Late Cenozoic deformation in the South Caspian region. Effects of a rigid basement block within a collision zone, *Tectonophysics* 366: 223-239.
- Allen MB, Jackson J, Walker R (2004) Late Cenozoic reorganization of the Arabia-Eurasia collision and the comparison of short-term and long-term deformation rates, *Tectonics* 23: 1-16.
- Alsharhan AS, Kendall CGSTC (2003) Holocene coastal carbonates and evaporites of the southern Arabian Gulf and their ancient analogues, *Earth Science Review* 61:191-243.
- Bathurst RGC (1975) Carbonate sediments and their diagenesis. Developments in sedimentology, volume 12: Elsevier, Amsterdam.
- Berberian M (1976) Contribution to the Seismotectonics of Iran (Part 2). Geological Survey of Iran.
- Bretis B, Grasemann B, Conradi F (2012) An active fault zone in the Western Kopeh Dagh (Iran), *Austrian Journal of Earth Sciences* 105/3: 95-107.
- Brigaud B, Durllet C, Deconinck JF, Vincent B, Thierry J, Trouiller A (2009) The origin and timing of multiphase cementation in carbonates: Impact of regional scale geodynamic events on the Middle Jurassic Limestones diagenesis (Paris Basin, France), *Sedimentary Geology* 222: 161-180.
- Budd DA (2001) Permeability loss with depth in the Cenozoic carbonate platform of west-central Florida, *American Association Petroleum Geologists Bulletin* 85: 1253-1272.
- Buryakovskiy LA, Chilingir GV, Aminzadeh F (2001) Petroleum Geology of the South Caspian Basin, Gulf Professional Publishing USA, 442pp.
- Carols LJ (2002) Diagenetic history of the Upper Jurassic Smackover Formation and its effects on reservoir properties: Vocation Field, Manila Sub-Basin, Eastern Gulf Coastal Plain, *Gulf Coast Assoc Geol Soc Trans* 52: 631-644.
- Chafetz HS, Alicia A, Imerito-Tetzalff J, Zhang J (1999) Stable-isotope and elemental trends in Pleistocene sabkha dolomites: descending meteoric water vs. sulfate reduction, *Journal of Sedimentary Research* 69: 256-266.
- Coffey BP, Read JF (2004) Mixed carbonate-siliciclastic sequence stratigraphy of paleogene transition zone continental shelf southeastern USA, *Sedimentary Geology* 166: 21-57.
- De Ros LF (1998) Heterogeneous generation and evolution of diagenetic quartzarenites in the Silurian-Devonian Fumas Formation of the Paran Basin, southern Brazil, *Sedimentary Geology* 116: 99-128.
- Dickinson WW, Milliken KL (1995) The diagenetic role of brittle deformation in compaction and pressure solution Etjo Sandstone Namibia, *Journal of Geology* 103: 339-347.
- Dunham RJ (1962) Classification of carbonate rocks according to depositional texture. In: Ham, W.E., (Ed.), Classification of carbonate rocks, *American Association Petroleum Geologists Memoir* 1: 108-121.
- Dutton SP, Diggs TN (1990) History of quartz cementation in the Lower Cretaceous Travis peak formation, East Texas, *Journal of Sedimentary Petrology* 60: 191-202.
- Ehrenberg SN, Pickard NAH, Svana TA, Oxtoby NH (2002) Cement geochemistry of photozoan carbonate strata (Upper Carboniferous- Lower Permian), Finnmark carbonate platform, Barents Sea, *Journal of Sedimentary Research* 72: 95-115.
- El-ghali MAK, Mansurbeg H, Morad S, Al-Aasm I, Ajdanlisky G (2006) Distribution of diagenetic alterations in fluvial and paralic deposits within sequence stratigraphic framework: Evidence from the Petrohan Terrigenous Group and the Svidol Formation, Lower Triassic, NW Bulgaria, *Sedimentary Geology* 190: 299-321.
- Ferry S, Pellenard P, Collin PY, Thierry J, Marchand D, Deconinck JF, Robin C, Carpentier C, Durllet C, Curial A (2007) Synthesis of recent stratigraphic data on Bathonian to Oxfordian deposits of the eastern Paris Basin, *Mémoire de la Société Géologique de France* 178: 37-57.
- Flügel E (1982) Microfacies Analysis of Limestones. Springer, Berlin, 633 pp.
- Flügel E (2004) Microfacies of Carbonate Rocks, Analysis, Interpretation and Application. Springer, Berlin, 967 PP.
- Flügel E (2010) Microfacies Analysis of Carbonate Rocks, Analyses, Interpretation and Application, Springer-verlag, Berlin, 976 pp.
- Folk RL (1965) Some aspects of recrystallization in ancient limestones. In: Pray, L.C., Murray, R.C., (Eds.), Dolomitization and Limestone Diagenesis, *Society of Economic Paleontologists and Mineralogists* 13: 14-48.
- Friis H, Sylvestersen RL, Nebel LN, Poulsen MLK, Svendsen JB (2010) Hydrothermally influenced cementation of sandstone — An example from deeply buried Cambrian sandstones from Bornholm, Denmark, *Sedimentary Geology* 227: 11-19.
- Garzanti E, Gaetani M (2002) Unroofing history of late Paleozoic magmatic arcs within the Turan Plate

- (Tuarkyr, Turkmenistan), *Sedimentary Geology* 151: 67-87.
- Giles MR, deBoer RB (1990) Origin and significance of redistributional secondary porosity, *Marine and Petroleum Geology* 6: 378-397.
- Girard JP, Munz IA, Johansen H, Lacharpagne JC, Sommer F (2002) Diagenesis of the Hild Brent sandstone, northern North Sea: isotopic evidence for the prevailing influence of deep basinal water, *Journal of Sedimentary Research* 72: 746-759.
- Götte T, Ramseyer K, Pettke T, Koch-Müller M (20013) Implications of trace element composition of syntaxial quartz cements for the geochemical conditions during quartz precipitation in sandstones, *Sedimentology* 60: 1111-1127.
- Hollingsworth J, Jackson J, Walker R, Gheitanchi MR, Bolourchi MJ (2006) Strike-slip faulting, rotation and along-strike elongation in the Kopet-Dagh Mountains, NE Iran, *Geophysical Journal International* 166: 1161-1177.
- Jackson J, Haines J, Holt W (1995) The accommodation of Arabia-Eurasia Plate convergence in Iran, *Journal of Geophysical Research*, 100: 205-215.
- Jackson J, Priestley K, Allen M, Berberian M (2002) Active tectonics of the South Caspian Basin, *Geophysical Journal International*, 148: 214-245.
- Kargaranbafghi F, Neubauer F, Genser J (2011) Cenozoic kinematic evolution of southwestern Central Iran: Strain partitioning and accommodation of Arabia-Eurasia convergence, *Tectonophysics* 502: 221-243.
- Kaviani A, Hatzfeld D, Paul A, Tatar M, Priestley K (2009) Shear-wave splitting, lithospheric anisotropy, and mantle deformation beneath the Arabia-Eurasia Collision Zone in Iran, *Earth and Planetary Science Letters* 286: 371-378.
- Kavoosi MA, Lasemi Y, Sherhati S, Moussavi-Harami R (2009) Facies analysis and depositional sequences of the Upper Jurassic Mozduran Formation, a carbonate reservoir in the Kopet-Dagh basin, NE Iran, *Journal of Petroleum Geology* 32(3): 235-260.
- Kyser TK, James NP, Bone I (2002) Shallow burial dolomitization of Cenozoic cool water limestone, southern Australia, Geochemistry and origin, *Journal of Sedimentary Research* 72: 146-157.
- Land LS (1984) Frio sandstone diagenesis, Texas Gulf Coast: a regional isotopic study. In: McDonald, D.A., Surdam, R.C., (Eds.), *Clastic Diagenesis*. Tulsa, Oklahoma, U.S.A. *American Association Petroleum Geologists Memoir* 37: 47-63.
- Lander RH, Walderhaug O (1999) Porosity prediction through simulation of sandstone compaction and quartz cementation, *American Association Petroleum Geologists Bulletin* 83: 433-449.
- Lasemi Y (1995) Platform Carbonates of the Upper Jurassic Mozduran Formation in the Kopet-Dagh Basin, NE Iran- facies paleoenvironments and sequences, *Sedimentary Geology* 99: 151-164.
- Lyberis N, Manby G (1999) Oblique to orthogonal convergence across the Turan Block in the post-Miocene, *American Association Petroleum Geologists Bulletin* 83: 1135-1160.
- Machent PG, Taylor KG, Macquaker JH, Marshall JD (2007) Pattern of early post-depositional and burial cementation in distal shallow marine sandstones: Upper Cretaceous Keniworth Member, Book Cliffs, Utah, USA, *Sedimentary Geology* 198: 125-145.
- Mahboubi A, Moussavi-Harami R, Lasemi Y, Brenner RL (2001) Sequence stratigraphy and sea level history of the upper Paleocene strata in the Kopet-Dagh Basin, northeastern Iran, *American Association Petroleum Geologists Bulletin* 85: 839-859.
- Mahboubi A, Moussavi-Harami R, Carpenter SJ, Aghaei A, Collins LB (2010) Petrographical and geochemical evidences for paragenetic sequence interpretation of diagenesis in mixed siliciclastic-carbonate sediments: Mozduran Formation (Upper Jurassic), south of Agh-Darband, NE Iran, *Carbonates Evaporites* 25: 231-246.
- Mansurbeg H, Morad S, Salem A, Marfil R, El-ghali MAK, Nystuen JP, Caja MA, Amorosi A, Garcia D, La Iglesia A (2008) Diagenesis and reservoir quality evolution of Palaeocene deep-water, marine sandstones, the Shetland-Faroes Basin, British continental shelf, *Marine and Petroleum Geology* 25: 514-543.
- Milliken KL (1994) The widespread occurrence of healed microfractures in siliciclastic rocks: evidence from scanned cathodoluminescence imaging. In: Nelson, P.P., Laubach, S.E., (Eds.), *Rock Mechanics: Models and Measurements, Challenges from Industry*, 1st North American Rock Mechanics Symposium, A.A. Balkema, pp. 825-832.
- Moussavi-Harami R (1989) Depositional history of Upper Jurassic (Oxfordian-Kimmeridgian) carbonates and evaporites in northeastern Iran (abs.). In: *Proceedings of the 28th international geological congress*, Washington DC, 2471 p
- Moussavi-Harami R, Brenner RL (1992) Geohistory analysis and petroleum reservoir characteristics of Lower Cretaceous (Neocomian) sandstones, eastern Kopet Dagh Basin, northeastern Iran, *American Association Petroleum Geologists Bulletin* 76: 1200-1208.
- North FK (1985) *Petroleum Geology*. Allen and Unwin, Boston, U.S.A., 607 pp.
- Palmer TJ, Hudson JD, Wilson MA (1988) Palaeoecological evidence for early aragonite dissolution in ancient seas, *Nature* 335: 809-810.
- Paxton ST, Szabo JO, Ajdukiewicz JM, Klimentidis RE (2002) Construction of an intergranular volume compaction curve for evaluating and predicting compaction and porosity loss in rigid-grain sandstone reservoirs, *American Association Petroleum Geologists Bulletin* 86: 2047-2067.

- Poursoltani MR, Moussavi-Harami R, Gibling MR (2007) Jurassic deep water fans in the Neo-Tethys Ocean, the Kashafrud Formation of the Kopet-Dagh Basin Iran, *Sedimentary Geology* 198: 53–74.
- Poursoltani MR, Gibling MR (2011) Composition, porosity and reservoir potential of the Middle Jurassic Kashafrud Formation northeast Iran, *Marine and Petroleum Geology* 28: 1094-1110.
- Purser BH (1969) Syn-sedimentary marine lithification of Middle Jurassic in the Paris Basin, *Sedimentology* 12: 205–230.
- Read JF (1985) Carbonate platform facies models, *American Association Petroleum Geologists Bulletin* 66: 860-878.
- Reilinger R, McClusky S, Vernant P, Lawrence S, Ergintav S, Ozener H, Kadirov F, Guliev I, Stepanyan R, Nadariya M, Hahubia G, Mahmoud S, Sakr K, Arrajehi A, Paradissis D, Al-Aydrus A, Prilepin M, Guseva T, Evren E, Dmitrova A, Filikov SV, Gomez F, Al-Ghazzi R, Karam G (2006) GPS constraints on continental deformation in the Africa-Arabia-Eurasia continental collision zone and implications for the dynamics of plate interactions, *Journal of Geophysical Research* 111, 26.
- Sanders D, Hofling R (2000) Carbonate deposition in mixed siliciclastic-carbonate environments on top of an orogenic wedge (Late Cretaceous, Northern Calcareous Alps, Austria), *Sedimentary Geology* 137: 127-146.
- Sardar Abadi M, Da Silva AC, Amini A, Aliabadi AA, Boulvain F, Sardar Abadi MH (2014) Tectonically controlled sedimentation: impact on sediment supply and basin evolution of the Kashafrud Formation (Middle Jurassic, Kopeh-Dagh Basin, northeast Iran), *International Journal of Earth Sciences* 103: 2233-2254.
- Schmid S, Worden RH, Fisher QJ (2004) Diagenesis and reservoir quality of the Sherwood Sandstone (Triassic), Corrib Field, Slyne Basin, west of Ireland, *Marine and Petroleum Geology* 21: 299-315.
- Scholle PA, Halley RB (1985) Burial diagenesis: out of sight, out of mind? In: Schneidermann, N., Harris, P.M., (Eds.), Carbonate Cements, *SEPM Special Publication* 36: 309–334.
- Shinn EA (1986) Modern carbonate tidal flats: their diagnostic features, *Quarterly Journal of Geol. Sch. Mines* 81: 7-35.
- Sibley DF, Gregg JM (1987) Classification of dolomite rock textures, *Journal of Sedimentary Petrology* 57: 967–975.
- Stöcklin J (1968) Structural history and tectonics of Iran: A review, *American Association Petroleum Geologists Bulletin* 52: 1229-1258.
- Taheri J, Fursich FT, Wilmsen M (2009) Stratigraphy, depositional environments and geodynamic significance of the Upper Bajocian-Bathonian Kashafrud Formation, NE Iran. In: Brunet, M.F., Wilmsen, M., Granath, J.W., (Eds.), Geological Society Special Publication, South Caspian to Central Iran Basins, London, UK, 312: 205-218.
- Tucker ME, Wright VP (1990) Carbonate Sedimentology, Blackwell, Oxford, 482 pp.
- Tucker ME (1993) Carbonate diagenesis and sequence stratigraphy. In: Wright, V.P., (Ed.), Sedimentary Review. Blackwell, Oxford, 208–226.
- Ulmishek G (2004) Petroleum geology and resources of the Amo-Darya Basin, Turkmenistan, Uzbekistan, Afghanistan, and Iran, *USGS Bull.* 32: 2201-4.
- Vernant P, Chery J (2006) Low fault friction in Iran implies localized deformation for the Arabia–Eurasia Collision Zone, *Earth and Planetary Science Letters* 246: 197-206.
- Vincent B, Emmanuel L, Houel P, Loreau JP (2007) Geodynamic control on carbonate diagenesis: petrographic and isotopic investigation of the Upper Jurassic formations of the Paris Basin (France), *Sedimentary Geology* 197: 267–289.
- Warren J (2006) Evaporites, Sediments, Resource and Hydrocarbons, Springer, Berlin, 1035 pp.
- Wilson JL (1975) Carbonate Facies in Geological History, Springer-Verlag, Berlin, 471 pp.
- Worden RH, Morad S (2000) Quartz cementation in oil field sandstones: a review of the key controversies. In: Worden, R.H., Morad, S., (Eds.), Quartz Cementation in Sandstones, *IAS Special Publication* 29: 1–20.
- Zand-Moghadam H, Moussavi-Harami R, Mahboubi A, Aghaei A (2016) Lithofacies and sequence stratigraphic analysis of the Upper Jurassic siliciclastics in the eastern Kopet-Dagh Basin, NE Iran, *Journal of African Earth Sciences* 117: 48-61.